Physics Letters A 380 (2016) 1641–1647

Contents lists available at ScienceDirect

Physics Letters A

www.elsevier.com/locate/pla

Temperature-dependent transformation thermotics for unsteady states: Switchable concentrator for transient heat flow

Ying Li [b,*], Xiangying Shen [a,*], Jiping Huang [a,*], Yushan Ni [b,*]

[a] Department of Physics, State Key Laboratory of Surface Physics, and Collaborative Innovation Center of Advanced Microstructures, Fudan University, Shanghai 200433, China
[b] Department of Mechanics and Engineering Science, Fudan University, Shanghai 200433, China

ARTICLE INFO

Article history:
Received 13 January 2016
Received in revised form 16 February 2016
Accepted 24 February 2016
Available online 27 February 2016
Communicated by R. Wu

Keywords:
Temperature-dependent transformation
Switchable concentrator
Thermal metamaterial
Effective medium theory

ABSTRACT

For manipulating heat flow efficiently, recently we established a theory of temperature-dependent transformation thermotics which holds for steady-state cases. Here, we develop the theory to unsteady-state cases by considering the generalized Fourier's law for transient thermal conduction. As a result, we are allowed to propose a new class of intelligent thermal metamaterial — switchable concentrator, which is made of inhomogeneous anisotropic materials. When environmental temperature is below or above a critical value, the concentrator is automatically switched on, namely, it helps to focus heat flux in a specific region. However, the focusing does not affect the distribution pattern of temperature outside the concentrator. We also perform finite-element simulations to confirm the switching effect according to the effective medium theory by assembling homogeneous isotropic materials, which bring more convenience for experimental fabrication than inhomogeneous anisotropic materials. This work may help to figure out new intelligent thermal devices, which provide more flexibility in controlling heat flow, and it may also be useful in other fields that are sensitive to temperature gradient, such as the Seebeck effect.

1. Introduction

Heat is one of the most common forms of energy in nature. To control heat flux and temperature gradient is both challenging and important. In recent years, many attempts have been made toward the possibility of manipulating thermal conduction to achieve desired temperature distribution or heat flux patterns [1–3], among which the approach with thermal metamaterials has won great successes.

In 2008, with the aforementioned attempt, Fan et al. [4] proposed steady-state transformation thermotics (or transformation thermodynamics) enlightened by the transformation optics established in 2006 [5,6], which has been successfully extended to other fields, such as acoustics waves [7–9], elastic waves [10], electric currents [11,12], and matter transport [13]. Later, originated from the steady-state and unsteady-state transformation thermotics [4, 14–18], researchers have designed plenty of thermal metamaterials with novel functions [19–27]. This method promises people to manipulate heat flow with more freedom by tailoring thermal conductivities of materials. It is long known that thermal conductivities vary with temperature, meaning a strong nonlinearity in the conduction equation (generalized Fourier equation). The existing theory of transformation thermotics does not take this effect into account until we recently put forward the theory of temperature-dependent transformation thermotics [28]. The new theory not only extended the existing transformation thermotics to a broader range of materials with temperature-dependent conductivities, but also offers a different tool to design devices with novel functions. However, our last work [28] only describes the steady-state cases, namely, the time-independent heat conduction process. Since the change of temperature distribution with time is always important in real applications, it becomes necessary to propose a temperature-dependent transformation thermotics which deals with the unsteady-state conduction equation. This is just an agenda of this work. Then, we take thermal concentrators as an example to show how the unsteady-state temperature-dependent transformation thermotics works. A thermal concentrator can help to raise the temperature gradient in a specific region, which, however, does not affect the pattern of temperature distribution outside the concentrator [19]. Here, we shall propose an intelligent concentrator, which can automatically be switched on or off as environmental temperature changes. Such a concentrator provides a different approach to non-invasively control the temperature gra-

* Corresponding authors.
E-mail addresses: 13110290008@fudan.edu.cn (Y. Li), 13110190068@fudan.edu.cn (X. Shen), jphuang@fudan.edu.cn (J. Huang), niyushan@fudan.edu.cn (Y. Ni).

http://dx.doi.org/10.1016/j.physleta.2016.02.040
0375-9601/

dient in real time, and thereby may help to adjust the efficiency of thermoelectric effects [29–31] or thermal energy harvesting cell [32] without unexpected interferences to the system. Also, it has other potential applications in heat preservation or energy-saving machines, and can be employed as building blocks in more complicated facilities.

2. Theory and design method

Our recently established theory of temperature-dependent (or nonlinear) transformation thermotics [28] only takes the steady-state thermal conduction into consideration. As a necessary extension, here we apply the theory on transient thermal conduction.

Consider the generalized Fourier's law for transient thermal conduction in n-dimension (without heat source),

$$\frac{\partial \rho c(T) T}{\partial t} = \nabla \cdot [\boldsymbol{\kappa}(T) \cdot \nabla T], \tag{1}$$

where ρ is the density, c is the specific heat capacity, and $\boldsymbol{\kappa}(T)$ is the thermal conductivity tensor which depends on temperature T. We take the multiply $\rho c(T)$ as a whole and assume it to be also temperature-dependent. By expressing Eq. (1) in a curvilinear coordinate system $(x^i, i = 1, \ldots, n)$ corresponding to a transformation, we have

$$\frac{\partial \rho c(T) T}{\partial t} = \frac{\partial}{\partial x^i} \kappa^{ij}(T) \frac{\partial}{\partial x^j} T + \Gamma^i_{ik} \kappa^{kj}(T) \frac{\partial}{\partial x^j} T, \tag{2}$$

where Γ^i_{ik} is the Christoffel symbol satisfying

$$\Gamma^i_{ik} = \frac{1}{2} g^{il} \frac{\partial}{\partial x^k} g_{il} = \det(J) \frac{\partial}{\partial x^k} \frac{1}{\det(J)}, \tag{3}$$

where g is the metric tensor, and J is the Jacobian matrix corresponding to the transformation. In order to rewrite Eq. (2) in the physical Cartesian coordinate system $(x'^i, i = 1, \ldots, n)$, we perform the variable change from x^i to the Cartesian coordinate x'^i and obtain

$$\begin{aligned} \frac{1}{\det(J)} \frac{\partial \rho c(T) T}{\partial t} &= \frac{\partial \det^{-1}(J) \rho c(T) T}{\partial t} \\ &= \frac{\partial}{\partial x'^i} \left[\frac{J \kappa(T) J^{\mathrm{t}}}{\det(J)} \right]^{ij} \frac{\partial}{\partial x'^j} T, \end{aligned} \tag{4}$$

where J^{t} and $\det(J)$ are respectively the transverse and the determinant of the Jacobian matrix J. We can see that the desired thermal conductivity $\tilde{\kappa}(T)$ is the same as that for the steady-state case

$$\tilde{\kappa}(T) = \frac{J \kappa(T) J^{\mathrm{t}}}{\det(J)}. \tag{5}$$

The additional requirement on the metamaterial for the transient case is that the multiply of its density $\tilde{\rho}$ and heat capacity $\tilde{c}$ should satisfy

$$\tilde{\rho} \tilde{c}(T) = \frac{\rho c(T)}{\det(J)}. \tag{6}$$

This requirement makes at least one of $\tilde{\rho}$ and $\tilde{c}$ a function of the spacial coordinates, and increases the difficulty in designing and realizing the device. Later, we shall present a convenient approach to handle this problem.

It is shown in our previous work [28] that $\tilde{\kappa}(T)$ can be expressed in the following form

$$\tilde{\kappa}(T) = \frac{\tilde{J}(T) \kappa_0 \tilde{J}(T)^{\mathrm{t}}}{\det[\tilde{J}(T)]}, \tag{7}$$

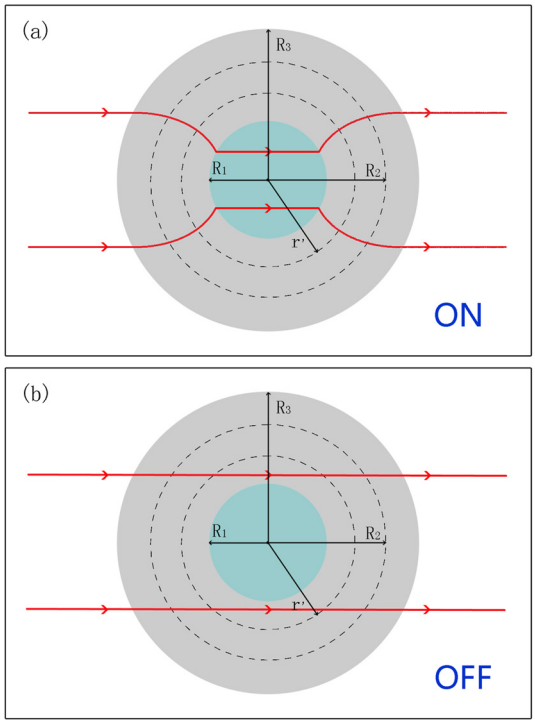

Fig. 1. Schematic graphs of a switchable thermal concentrator when the concentrating effect is switched (a) on or (b) off. The red lines with arrows represent the flow of heat. R_1 and R_3 denote the interior radius and exterior radius, respectively. R_2 and r' are also indicated, whose meaning can be found in the text. (For interpretation of the references to color in this figure legend, the reader is referred to the web version of this article.)

where $\tilde{J}(T)$ is the Jacobian matrix corresponding to a transformation which varies with temperature, and κ_0 is a constant temperature-independent thermal conductivity. Similarly, we can also have

$$\tilde{\rho} \tilde{c}(T) = \frac{\rho_0 c_0}{\det[\tilde{J}(T)]}, \tag{8}$$

where ρ_0 and c_0 are temperature-independent density and heat capacity, respectively. Based on the above expressions, we are able to make a thermal metamaterial behave differently at different environmental temperatures. As a demonstration, we introduce the concept of switchable thermal concentrator.

The function of a thermal concentrator is schematically plotted in Fig. 1(a), where a polar coordinate system (r', θ') is constructed. The device is the gray ring with interior radius R_1 and exterior radius R_3. It guides heat flux (indicated with red lines with arrows) to travel through its inner region $(r' < R_1)$, and thus increases the temperature gradient inside it without disturbing the temperature distribution of the background $(r' > R_3)$. As researchers have proved [15,19], this function can be achieved by using a transformation, $r' = f(r)$ and $\theta' = \theta$, where

$$r' = f(r) = \begin{cases} r \frac{R_1}{R_2}, & r' < R_1 \\ r \frac{R_3 - R_1}{R_3 - R_2} + R_3 \frac{R_1 - R_2}{R_3 - R_2}, & R_1 \le r' \le R_3 \end{cases}. \tag{9}$$

Here, R_2 is a constant parameter that satisfies $R_1 < R_2 < R_3$. Based on the original idea of a thermal concentrator, the switchable thermal concentrator is a device which only functions at certain temperature range. For example, the device can be designed to function as a normal thermal concentrator when environmental temperature is lower (or higher) than a critical temperature T_c, but have no influence on the field profile when temperature is beyond (or below) T_c.

The switching effect can be realized by revising Eq. (9). It is noticed that an identical mapping, $r' = r$ and $\theta' = \theta$, does not affect the temperature distribution or the heat flux, and by replacing R_2 in Eq. (9) with R_1 we get exactly the identical mapping. Therefore we construct a function $R^*(T)$ which approaches R_2 as T decreases below T_c and approaches R_1 as T increases above T_c. One convenient form of $R^*(T)$ with such properties is

$$R^*(T) = R_1 + (R_2 - R_1)/\left[1 + e^{\beta(T-T_c)}\right], \tag{10}$$

where β is a scaling factor. The new transformation for the switchable thermal concentrator is then $r' = F(r, T)$ and $\theta' = \theta$, where

$$F(r,T) = \begin{cases} r\frac{R_1}{R^*(T)}, & r' < R_1 \\ r\frac{R_3 - R_1}{R_3 - R^*(T)} + R_3\frac{R_1 - R^*(T)}{R_3 - R^*(T)}, & R_1 \le r' \le R_3 \end{cases}. \tag{11}$$

Next, the desired the thermal conductivity distribution of the device can be calculated according to Eq. (7). The results written in the polar coordinate system are

$$\begin{cases} \tilde{\kappa}_r(T) = \kappa_0, \\ \tilde{\kappa}_\theta(T) = \kappa_0, & r' < R_1 \\ \tilde{\kappa}_r(T) = \kappa_0\left[1 + \frac{R_3}{r'}\frac{R^*(T) - R_1}{R_3 - R^*(T)}\right], \\ \tilde{\kappa}_\theta(T) = \kappa_0\left[1 + \frac{R_3}{r'}\frac{R^*(T) - R_1}{R_3 - R^*(T)}\right]^{-1}, & R_1 \le r' \le R_3, \end{cases} \tag{12}$$

where κ_0 is the constant temperature-independent thermal conductivity of the background and the inner region.

The temperature-dependent transformation thermotics for transient thermal conduction has requirements not only on the thermal conductivity, but also on the density and heat capacity of the metamaterial, as expressed in Eq. (8). As for the switchable thermal concentrator, we have

$$\frac{\rho_0 c_0}{\det[\tilde{J}(T)]} = \begin{cases} \left[\frac{R^*(T)}{R_1}\right]^2, & r' < R_1 \\ \left[1 + \frac{R_3}{r'}\frac{R^*(T) - R_1}{R_3 - R^*(T)}\right]\left[\frac{R_3 - R^*(T)}{R_3 - R_1}\right]^2, & R_1 \le r' \le R_3. \end{cases} \tag{13}$$

It is noticed that although the thermal conductivity of the inner region is not changed according to Eq. (12), the density or heat capacity of the inner region should be modified. This fact introduces additional difficulty. To overcome these problems about $\tilde{\rho}\tilde{c}$, we propose an approximate approach which keeps $\tilde{\rho}\tilde{c}(T) = \rho_0 c_0$. Unlike the widely used approach for transient thermal cloaking [15,16], it is suggested that no modification is applied on the thermal conductivity of the switchable thermal concentrator. The reason is that for a concentrator when $R^*(T)$ approaches R_2, $\det^{-1}[\tilde{J}(T)]$ in the whole region ($r' \le R_3$) averages to be one,

$$\frac{\int_0^{R_3} \det^{-1}[\tilde{J}(T)] 2\pi r' dr'}{\pi R_3^2} = \frac{1}{\pi R_3^2}\left[\int_0^{R_1}\left(\frac{R_2}{R_1}\right)^2 2\pi r' dr' + \int_{R_1}^{R_3}\left(1 + \frac{R_3}{r'}\frac{R_2 - R_1}{R_3 - R_2}\right)\left(\frac{R_3 - R_2}{R_3 - R_1}\right)^2 2\pi r' dr'\right] = 1. \tag{14}$$

Also when the concentrating effect is switched off as $R^*(T)$ approaches R_1, $\det^{-1}[\tilde{J}(T)] = 1$ at any space point and no modification is required for the density or heat capacity.

3. Results and discussion

After introducing the design of the switchable thermal concentrator, we perform finite element simulations with the commercial software COMSOL Multiphysics to see how the device works at different environmental temperatures. Without loss of generality, we adopt nondimensionalized units in our simulations. The units of length, temperature, thermal conductivity and time are defined as $L_x/8$ (L_x is the width of the simulation box), the initial temperature, the conductivity of background κ_0 and $L_x^2\rho c/64\kappa_0$, respectively. A ring with interior radius $R_1 = 1$ and exterior radius $R_3 = 3$ is set in a box with size 8×7 as shown in Fig. 1, and the parameter R_2 is set as 2. Heat conducts from the left boundary with high temperature T_H to the right boundary with low temperature T_L, while the upper and lower boundaries of the simulation box are thermally isolated.

The simulation results of the time-dependent heat conduction through the device are shown in Fig. 2. The critical temperature T_c is set to be 1. According to the discussion aforementioned, the density ρ_0 and heat capacity c_0 are both constant and also nondimensionalized to the value of 1. In Fig. 2(a)–(d), when the temperature is low ($T = 0.7 \sim 0.9$), we see that the device functions as a concentrator throughout the whole simulation time ($t = 0 \sim 14$), and the heat flow is focused in the core region, where the temperature gradient is raised. On the other hand, when the boundary temperatures are high enough ($T = 1.1 \sim 1.3$), the concentrating effect is "turned off" during the same simulation time (Fig. 3(e)–(h)). The heat diffuses from left to right as if the device is absent. It should be noted that although the factor ρc is not multiplied by $\det(J)$, the approximation seems to be good enough since the disturbances to the external temperature distribution are inconspicuous. Due to the antisymmetry, a switchable concentrator that only functions at high temperature can also be figured out in the same way.

The thermal conductivity of such a thermal metamaterial is inhomogeneous and anisotropic. As a suggestion for further experiment, we resort to the effective medium theory (EMT) [33,14,34] by using a multi-layered structure. The concentric structure is consisted with alternating layers of two different homogeneous isotropic materials with conductivities $\kappa_A(T)$ and $\kappa_B(T)$ to achieve a compression transformation effect. This method has been applied successfully in the experiments of thermal cloaks based on transformation thermotics [19,16]. For the extension transformation, the orientation of the two layers should be rotated an angle of $\pi/2$. Thus, the compression can be approximated by arraying alternating layers along radial direction, and the extension is achieved by such arrays along the azimuthal direction. Therefore, considering both two transformations, the switchable concentrator is divided into 400 grids as shown in Fig. 3. According to the EMT, for each alternating unit layer, which is consisted of two homogeneous isotropic sub-layers, the following relations exist for the effective parameters,

$$\frac{1}{\kappa_r(T)} = \frac{1}{1+\eta}\left(\frac{1}{\kappa_A(T)} + \frac{\eta}{\kappa_B(T)}\right), \qquad \kappa_\theta(T) = \frac{\kappa_A(T) + \eta\kappa_B(T)}{1+\eta}, \tag{15}$$

where $\eta = d_B/d_A$. In this work, we set $\eta = 1$.

The above equation is reliable in realizing the theoretical design. However, the resulting forms of $\kappa_A(T)$ and $\kappa_B(T)$ derived from Eq. (15) are so complex that they are hard to be realized experimentally. For simplification, we propose that instead of get-

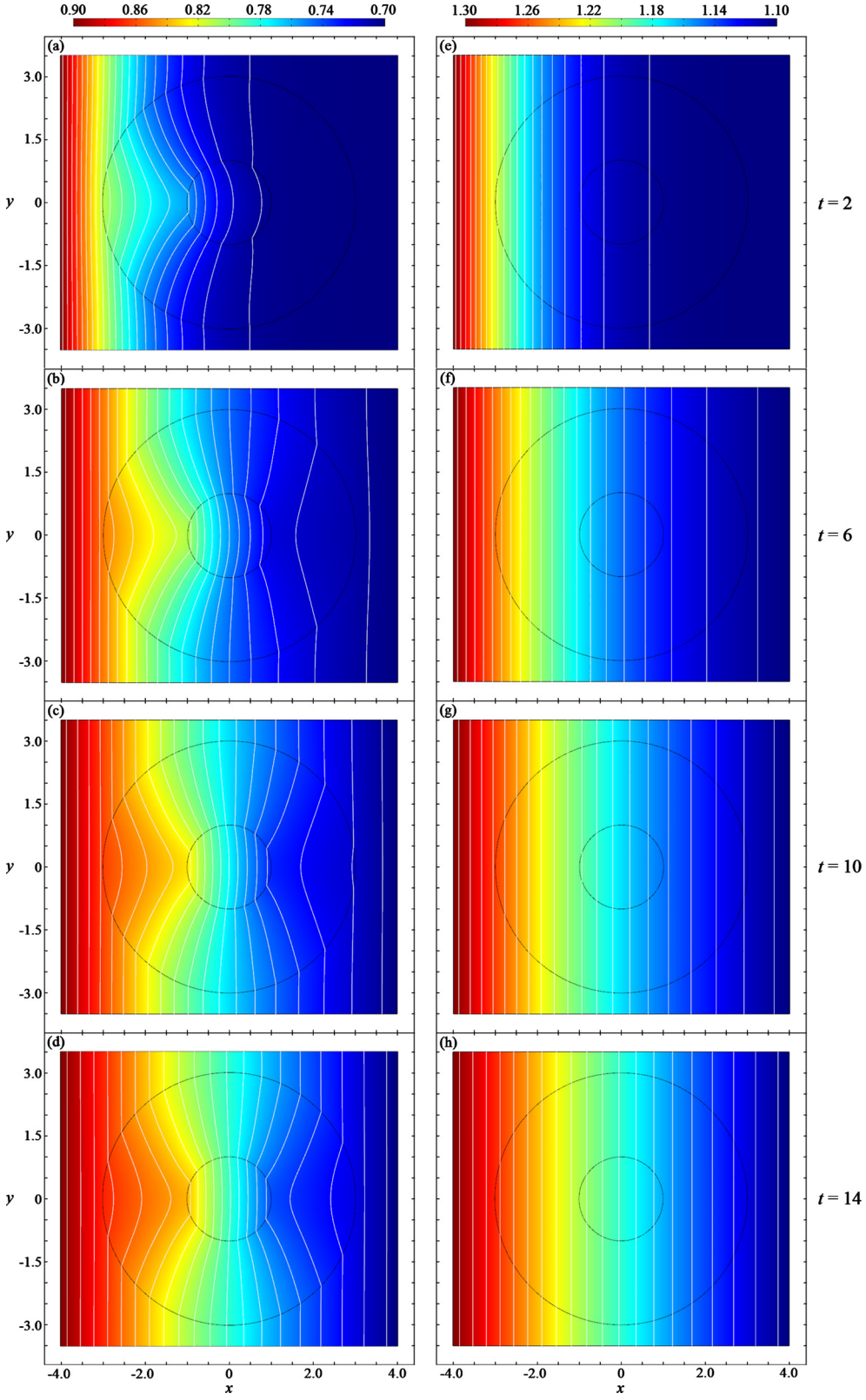

Fig. 2. Results of the finite-element simulations for the switchable concentrator. All the physical quantities adopted are nondimensionalized, as listed in the text. Heat conducts from left to right throughout the time and the temperatures on two lateral boundaries are fixed. Upper and lower boundaries are thermally insulated. The critical temperature T_c is set to be 1. (a–d) The device functions as a concentrator at temperature below 0.9 and (e–h) the device is turned to be the same as the background when the temperature is higher than 1.1. The temperature distribution is denoted by the rainbow color surfaces, while the isothermal lines are indicated by the white lines. We take the snapshots of temperature distributions at time (a, e) $t = 2$, (b, f) $t = 6$, (c, g) $t = 10$, and (d, h) $t = 14$. (For interpretation of the references to color in this figure legend, the reader is referred to the web version of this article.)

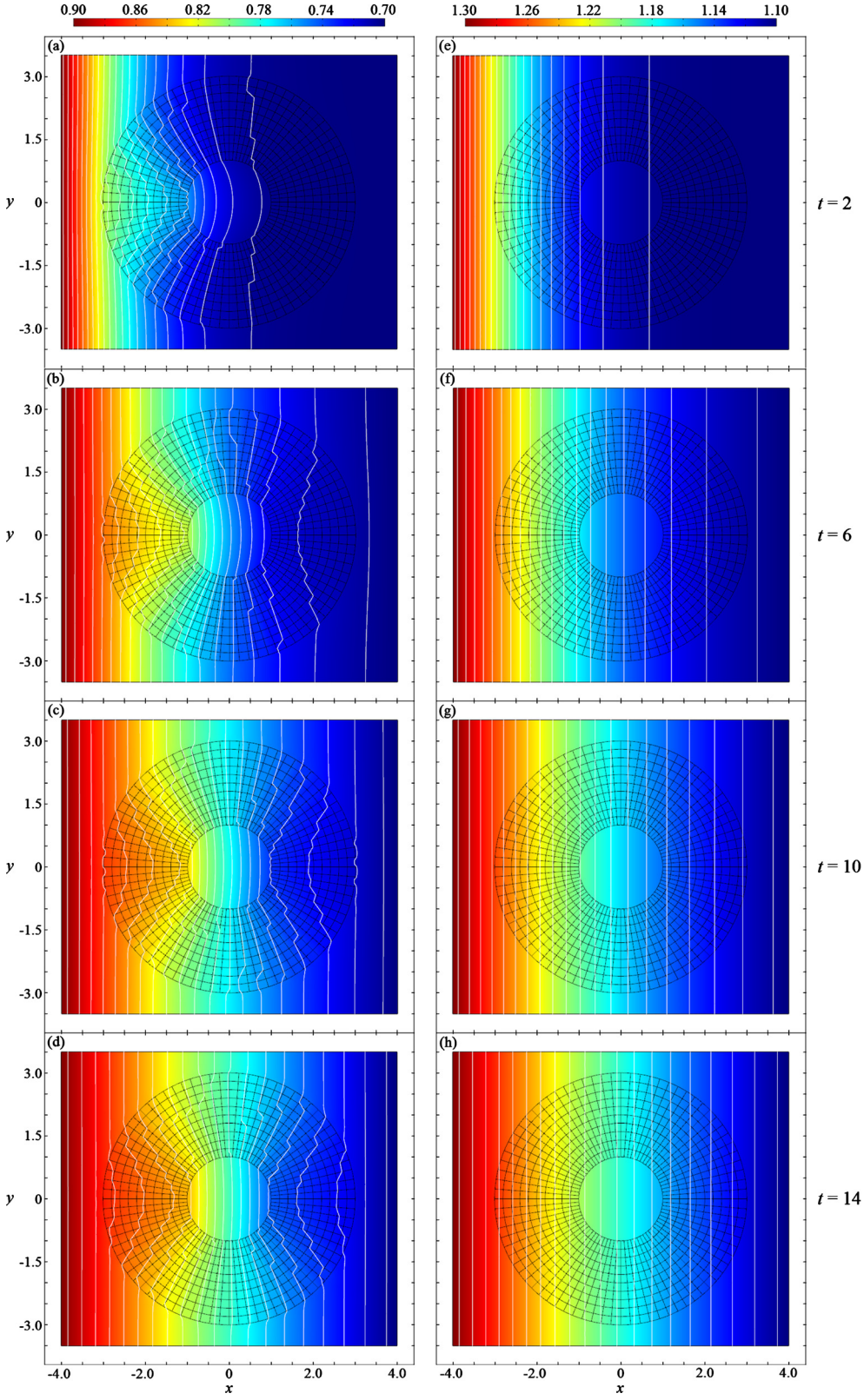

Fig. 3. Results of the finite-element simulations for the multi-layered switchable concentrator with 400 grids. The parameters of each grid can be obtained from Eq. (16) and Eq. (17). We take the snapshots of temperature distributions at the same time as Fig. 2. Compared to Fig. 2, the behaviors of the device assembled based on the EMT are in agreement with the theoretical model. (For interpretation of the references to color in this figure legend, the reader is referred to the web version of this article.)

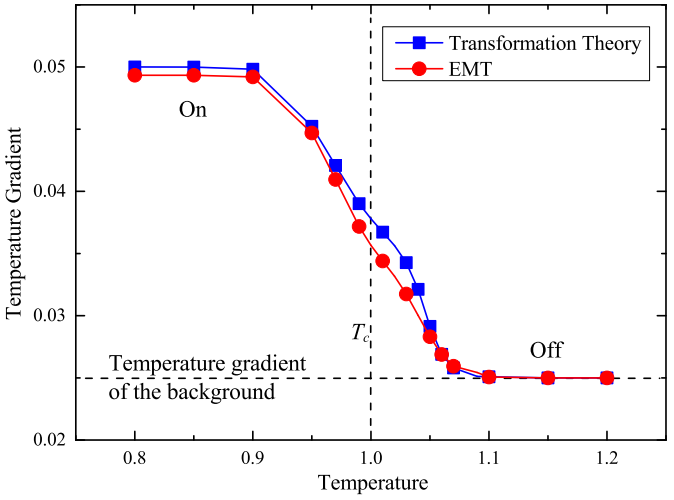

Fig. 4. Temperature gradients within the central region (i.e., the region with a radius smaller than R_1) along x direction at different environmental temperatures (defined as the average temperature of the heat and cold sources). As shown in the figure, the blue squares and red circles denote the simulation results based on the unsteady-state temperature-dependent transformation theory and the EMT, respectively. The x-direction temperature gradient of the background remains constant and is noted with the horizontal dashed line, while the critical temperature T_c is indicated with the vertical dashed line. (For interpretation of the references to color in this figure legend, the reader is referred to the web version of this article.)

ting the thermal conductivities directly from Eq. (15), we solve the limiting case of a normal concentrator,

$$\frac{1}{\kappa_r} = \frac{1}{2}\left(\frac{1}{\kappa_A} + \frac{1}{\kappa_B}\right), \qquad \kappa_\theta = \frac{\kappa_A + \kappa_B}{2}, \tag{16}$$

where κ_r and κ_θ are the original temperature-independent conductivities. Then the desired $\kappa_A(T)$ and $\kappa_B(T)$ can be simply expressed by the temperature-involved factors and solutions of Eq. (16):

$$\kappa_{A(B)}(T) = 1 + \frac{\kappa_{A(B)} - 1}{\left[1 + e^{\beta(T-T_c)}\right]}. \tag{17}$$

The above temperature-dependent conductivity exhibits a sharp switch between two values as temperature varies, which can be directly achieved through phase-change materials [35] or effectively through shape-memory alloys [36] or shape-memory polymers [37].

After obtaining $\kappa_A(T)$ and $\kappa_B(T)$, we are now in a position to test the facility. Under the same simulation conditions, the switching effect of concentrator is presented in Fig. 3. Obviously, the device based on the EMT works as well as the theoretical design.

For clarity, in Fig. 4, the temperature gradient within the device is displayed to reflect the effects of switchable thermal concentrator. High values of temperature gradient indicate that the concentrating effect is activated. Under different boundary conditions of temperature, the variations of the temperature gradients of both the theoretical model and the EMT model are shown in Fig. 4. As shown in the figure, the thermal metamaterial is sensitive to the environmental temperature, and it is thus called intelligent thermal metamaterials. In particular, the transition process which happens around the critical point T_c ($T_c = 1$) is sharp. It is also seen that the results based on the EMT are in agreement with those based on the transformation theory.

4. Conclusions

We have extended the theory of temperature-dependent transformation thermotics to unsteady-state cases by taking into account the transient thermal conduction equation. As a result, we have proposed a kind of switchable thermal concentrator. This concentrator can be switched on as a normal thermal concentrator when environmental temperature is below (or above) a certain critical temperature, and it can be automatically turned off when the environmental temperature reaches a value higher (or lower) than the critical temperature. With time-dependent simulations, we have shown that the requirements on density and heat capacity for transient thermal concentrating can be approximately handled by simply keeping their original values, which doesn't introduce significant distortion of the temperature field outside the device. The switchable concentrating effect has also been achieved with the structure constructed by assembling homogeneous isotropic materials according to the EMT (effective medium theory). It suggests a viable way for experimental realization of the device with materials whose thermal conductivities are temperature sensitive such as various kinds of phase-change materials [35–37]. The effect of the switchable thermal concentrator has been quantitatively studied by calculating the temperature gradient within its inner region for different temperature fields. The results based on the nonlinear theory and the EMT have both showed a sharp decrease of the temperature gradient near the critical temperature, indicating a quick response of our device to the change of environmental temperature.

Acknowledgements

We acknowledge the financial support by the National Natural Science Foundation of China under Grants No. 11222544 and No. 11572090 (Y.L. and Y.N.), by the Fok Ying Tong Education Foundation under Grant No. 131008, by the Program for New Century Excellent Talents in University (NCET-12-0121), and by the CNKBRSF under Grant No. 2011CB922004.

Y.L. and X.S. contributed equally to this work.

Appendix A. Supplementary material

Supplementary material related to this article can be found online at http://dx.doi.org/10.1016/j.physleta.2016.02.040.

References

[1] N. Li, J. Ren, L. Wang, G. Zhang, P. Hanggi, B. Li, Rev. Mod. Phys. 84 (2012) 1045.
[2] F. Giazotto, M.J. Martínez-Pérez, Nature 492 (2012) 401.
[3] M. Maldovan, Nature 503 (2013) 209.
[4] C.Z. Fan, Y. Gao, J.P. Huang, Appl. Phys. Lett. 92 (2008) 251907.
[5] U. Leonhardt, Science 312 (2006) 1777.
[6] J.B. Pendry, D. Schurig, D.R. Smith, Science 312 (2006) 1780.
[7] S. Zhang, C. Xia, N. Fang, Phys. Rev. Lett. 106 (2011) 024301.
[8] X.L. Zhang, X. Ni, M.H. Lu, Y.F. Chen, Phys. Lett. A 376 (2012) 493–496.
[9] L. Zigoneanu, B. Popa, S.A. Cummer, Nat. Mater. 13 (2014) 352.
[10] T. Bückmann, M. Thiel, M. Kadic, R. Schittny, M. Wegener, Nat. Commun. 5 (2014) 4130.
[11] L.W. Zeng, Phys. Lett. A 378 (2014) 923–926.
[12] S. Savo, Y. Zhou, G. Castaldi, M. Moccia, V. Galdi, S. Ramanathan, Y. Sato, Phys. Rev. B 91 (2015) 134105.
[13] R. Schittny, M. Kadic, T. Bückmann, M. Wegener, Science 345 (2014) 427.
[14] J.Y. Li, Y. Gao, J.P. Huang, J. Appl. Phys. 108 (2010) 074504.
[15] S. Guenneau, C. Amra, D. Veynante, Opt. Express 20 (2012) 8207.
[16] R. Schittny, M. Kadic, S. Guenneau, M. Wegener, Phys. Rev. Lett. 110 (2013) 195901.
[17] H. Xu, X. Shi, F. Gao, H. Sun, B. Zhang, Phys. Rev. Lett. 112 (2014) 054301.
[18] T. Han, X. Bai, D. Gao, J.T.L. Thong, B. Li, C.W. Qiu, Phys. Rev. Lett. 112 (2014) 054302.
[19] S. Narayana, Y. Sato, Phys. Rev. Lett. 108 (2012) 214303.
[20] Y. Gao, J.P. Huang, Europhys. Lett. 104 (2013) 44001.
[21] S. Guenneau, C. Amra, Opt. Express 21 (2013) 6578.
[22] Y. Ma, Y. Liu, M. Raza, Y. Wang, S. He, Phys. Rev. Lett. 113 (2014) 205501.
[23] X.Y. Shen, J.P. Huang, Int. J. Heat Mass Transf. 78 (2014) 1.
[24] T. Han, X. Bai, J.T.L. Thong, B. Li, C.W. Qiu, Adv. Mater. 26 (2014) 1731.
[25] T. Yang, X. Bai, D. Gao, L. Wu, B. Li, J.T.L. Thong, C-W. Qiu, Adv. Mater. 27 (2015) 7752.

[26] T. Han, C-W. Qiu, Transformation Laplacian metamaterials: recent advances in manipulating thermal and dc fields, J. Opt. (2016), in press.
[27] Y. Ma, M. Raza, Y. Liu, E-H. Lee, Transformation thermodynamics and heat cloaking: a review, J. Opt. (2016), in press.
[28] Y. Li, X.Y. Shen, Z.H. Wu, J.Y. Huang, Y.X. Chen, Y.S. Ni, J.P. Huang, Phys. Rev. Lett. 115 (2015) 195503.
[29] K. Uchida, S. Takahashi, K. Harii, J. Ieda, W. Koshibae, K. Ando, S. Maekawa, E. Saitoh, Nature (London) 455 (2008) 778.
[30] M. Wang, C. Bi, L. Li, S.B. Long, Q. Liu, H.B. Lv, N.H. Lu, P.X. Sun, M. Liu, Nat. Commun. 5 (2014) 4598.
[31] S.M. Wu, J.E. Pearson, A. Bhattacharya, Phys. Rev. Lett. 114 (2015) 186602.
[32] T. Han, J. Zhao, T. Yuan, D.Y. Lei, B. Li, C-W. Qiu, Energy Environ. Sci. 6 (2013) 3537.
[33] J.P. Huang, K.W. Yu, Phys. Rep. 431 (2006) 87.
[34] Y. Gao, J.P. Huang, Y.M. Liu, L. Gao, K.W. Yu, X. Zhang, Phys. Rev. Lett. 104 (2010) 034501.
[35] R. Zheng, J. Gao, J. Wang, G. Chen, Nat. Commun. 2 (2011) 289.
[36] C. Chluba, W. Ge, R.L. Miranda, J. Strobel, L. Kienle, E. Quandt, M. Wuttig, Science 348 (2015) 1004.
[37] Q. Zhao, H.J. Qi, T. Xie, Prog. Polym. Sci. 49–50 (2015) 79.